Received: 2 July 2019 | Revised: 29 August 2019 | Accepted: 1 September 2019
DOI: 10.1002/aoc.5250

FULL PAPER

WILEY Applied Organometallic Chemistry

Pulsed laser ablated zeolite nanoparticles: A novel nanocatalyst for the synthesis of 1,8-dioxo-octahydroxanthene and *N*-aryl-1,8-dioxodecahydroacridine with molecular docking validation

A.M. Abdelghany[1,2] | **A.A. Menazea**[1,3] | **Mansoura A. Abd-El-Maksoud**[4] | **Tamer K. Khatab**[4]

[1] Spectroscopy Department, Physics Division, National Research Centre, 33 ElBehouth Street, PO Box 12622, Dokki, Giza, Egypt

[2] Basic Science Department, Horus University, International Coastal Road, New Damietta, KafrSaad, Damietta, Egypt

[3] Laser Technology Unit, National Research Centre, 33 ElBehouth Street, PO Box 12622, Dokki, Giza, Egypt

[4] Organometallic and Organometalloid Chemistry Department, National Research Centre, 33-El-Buhouth Street, PO Box 12622, Dokki, Giza, Egypt

Correspondence
A. M. Abdelghany, Spectroscopy Department, Physics Division, National Research Centre, 33 ElBehouth Street, PO Box 12622, Dokki, Giza, Egypt.
Email: a.m_abdelghany@yahoo.com

There is an increasing interest in the synthesis of metal nanoparticles (NPs) from bulk metals using pulsed laser ablation in liquids (PLAL), as it offers an easy and simple synthesis route. In this work, zeolite NPs (molecular sieve 4A) were successfully synthesized by the PLAL technique, and characterized by X-ray diffraction, scanning electron microscopy, Fourier transform infrared spectroscopy, transmission electron microscopy, field emission scanning electron microscopy, and high-resolution transmission electron microscopy. Data obtained confirm the formation of the crystalline phase of zeolite. The synthesized catalyst (zeolite molecular sieve 4A) was used as an efficient and facile promotor for the synthesis of xanthene and acridine derivatives. Molecular docking of the synthesized compounds was validated using quinone reductase 2 (NQO2) and acridine orange as the ligand, with the synthesized molecules showing good drug–ligand interaction on the active site of NQO2, compared with that of acridine orange.

KEYWORDS
acridine, dimedone, laser ablation, nanoparticles, xanthene, zeolite

1 | INTRODUCTION

Zeolite is a microporous and aluminosilicate mineral used as a molecular sieve and as an adsorbent of several cations, such as Ca^{2+}, K^{+}, Na^{+}, and Mg^{2+}.[1] It is also applied in the modification of several bioreactor devices.[2] Zeolite (molecular sieve 4A) is an alkali metal aluminosilicate. Molecular sieve 4A is the sodium form of the type A crystal structure of zeolite, and can adsorb molecules with diameters smaller than 4 Å (0.4 nm).

Zeolite (molecular sieve 4A) is produced by the reaction of water, sodium silicate, sodium aluminate, and sodium hydroxide. Molecular sieve 4A is usually packed in small bags for use in packaging of desiccant foods, electronic components, and drugs. It is also used for drying and removing of CO_2 from natural gas, liquefied petroleum gas, or air, and for the removal of hydrocarbons, ammonia, and methanol from gas streams (ammonia syn gas treating) and for dehydration of refrigeration systems and air streams in the air-break units of buses, trucks, and locomotives.[3–6]

In recent years, nanoparticles (NPs) have attracted wide attention due to their excellent physical and chemical properties and appear promising in the field of material science.[7–11] Subjecting metal NPs to pulsed laser ablation of solids in liquids environment (PLAL)

https://doi.org/10.1002/aoc.5250

is one of the promising routes to obtain metal colloids. PLAL has received much attention as a novel technique for synthesizing NPs. NPs of various species of materials such as metals, metal oxides, semiconductors, and organic materials can be obtained by irradiating intense nanosecond laser onto these materials settled in solvents.[12–14] This is a fast, simple, straightforward, and easy method to prepare NPs compared with other methods.

Several methods for producing xanthenes and acridines have been reported in the literature, as these organic compounds exhibit a wide range of pharmaceutical activity and have industrial and synthetic applications.[15–23] Catalytic condensation of dimedone and variable aldehydes is a common method for the synthesis of xanthenes such as polyphosphoric acid (PPA)–SiO_2,[24] $SbCl_3$–SiO_2,[25] silica sulfate,[26] $NaHSO_4 \cdot SiO_2$,[27] and $ZrOCl_2 \cdot 8H_2O$.[28] By contrast, acridines could be synthesized by mixing aromatic aldehydes, dimedone, and nitrogen sources such as urea,[29] aniline,[30] ammonium acetate,[31] hydroxyl amines,[32] ammonium hydroxide, and ammonium bicarbonate.[33] The aforesaid syntheses reactions have been achieved using various catalysts such as amberlyst-15,2,3–Dicyano–1,4–hydroquinone (DCH), DBH[34]; Nano CeO_2[35]; ammonium chloride or L-proline, $Zn(OAc)_2 \cdot 2H_2O$[36]; nano-Fe_3O_4@SiO_2-SO_3H[37]; SO_4^{2-}/ZrO_2[38]; ionic liquids[39]; b-cyclodextrin[40]; and imidazolium salts with perfluoroalkyl tails such as Bronsted acid.[41] Unfortunately, most available methods have many disadvantages, such as the use of corrosive, expensive, and not easily available reagents and require drastic reaction conditions such as refluxing, strong acidic medium, and fatiguing Reaction work-up boundaries.

To overcome these disadvantages, we herein propose a catalytic synthesis of xanthenes and acridines over an efficient and recyclable catalyst, zeolite (molecular sieve 4A), which was prepared by a novel method (laser ablation). The obtained structures of xanthenes, acridines, and zeolite were characterized and analyzed by scanning electron microscopic (SEM) measurements, X-ray diffraction (XRD) scans, and Fourier transform infrared (FT-IR) spectra.

2 | EXPERIMENTAL

2.1 | Catalyst preparation

2.1.1 | Materials

Zeolite [molecular sieve 4A; CAS No.: 1318-02-1; chemical formula: $Na_2O \cdot Al_2O_3 \cdot 2SiO_2 \cdot 4, 5H_2O$, silica-to-alumina ratio (SiO_2/Al_2O_3) ≈ 2] was purchased from Sigma-Aldrich and used without further purification. Deionized water was used as the solvent media for laser ablation.

2.1.2 | Synthesis of zeolite 4A nanoparticles by PLAL

Zeolite NPs were prepared by PLAL. First, a zeolite plate (target) of high purity (99.99%; dimensions: 10 mm diameter and 3 mm thickness) was placed at the bottom of a beaker filled with 30 ml deionized water solution. The height of the solution was 1.5 cm from the target plate. The target was irradiated with Nd:YAG nanosecond pulsed laser (PRII 8000 Continuum laser; Electro–optics, Inc.) under the following conditions: fundamental wavelength of 1064 nm with 4 W power, 10 Hz pulse repetition rate, and 7 nm pulse width for 20 min. The laser beam was incident perpendicularly on the surface of the plate target after focusing it through a 10-cm focal length convex lens to achieve laser ablation on the surface of the target.

2.1.3 | Characterization

The crystalline structure of samples was characterized using PANalytical X'Pert Pro XRD diffractometer system with Cu-Kα radiation (λ = 0.154 nm) operating at 45 kV. All scans were performed over a 2θ range from 4° to 80° under UV–Vis light. Optical measurements were studied as a function of wavelength λ (nm) of the prepared samples and measured using a JASCO (V-570) UV/VIS/NIR double-beam spectrophotometer at room temperature at the wavelength region between 200 and 1000 nm.

FT-IR was used to demonstrate the chemical composition of samples prepared. FT-IR spectral data were collected through 32 scans with resolution of 2 cm^{-1} using a single-beam spectrometer (Nicolet iS 10) via the KBr powder route at wavenumbers between 4000 and 400 cm^{-1} and their structures examined. The morphology and topography of the samples prepared were analyzed by field emission scanning electron microscopy (FE-SEM; Quanta FEG 250) and high-resolution transmission electron microscope (HR-TEM; JEOL-JEM-1011). Synthesized Materials was investigated by energy-dispersive X-ray spectroscopy using the software (TEAM) built into the scanning electron microscope (Quanta FEG 250 electron microscope).

2.2 | Chemicals apparatus

The nuclear magnetic resonance (NMR) instrument used for the illustration of organic compounds was Joel 500 MHz spectrometer in $CDCl_3$. The measuring unit of chemical shifts (δ) is parts per million (ppm). Mass spectra were recorded on an Agilent LC–MS spectrometer (pump quaternary 1200 Series; quadruple MSD 6110). Reaction monitoring by thin-layer chromatography (TLC) was performed on Merck silica gel GF254 plates and visualized by UV light (254 nm). All chemicals were obtained from Sigma-Aldrich.

2.2.1 | Structure elucidation and general procedure

1. A mixture of aldehydes (1 mmol), dimedone (2 mmol), and modified to (ZNps, 10 mol%) was stirred at 60–70 °C. The reaction mixture was followed by TLC until the substrates disappeared. Chloroform (20 ml) was used to extract the organic product and the pure products were obtained after recrystallization.

2. A mixture of aldehydes (1 mmol), dimedone (2 mmol), various anilines (1 mmol), and modified to (ZNps, 10 mol%) was stirred at 60–70 °C. The reaction mixture was followed by TLC until the substrates disappeared. Chloroform (20 ml) was used to extract the organic product.

2.2.2 | Structure elucidation data of new compounds

10-(Benzo[d][1,3]dioxol-5-yl)-3,4,6,7-tetrahydro-9-(3-pyridyl)-3,3,6,6 tetramethylacridine-1,8(2H,5H,9H,10H)-dione (5d)

IR (KBr): 1620 (C=O), 1615 (C=O) cm^{-1}, ^1H-NMR (400 MHz, $CDCl_3$) δ ppm: 0.96–1.04 (s, $4CH_3$), 2.16, 2.20 (s, $2CH_2$), 2.47 (d, CH), 2.50 (d, CH), 4.95 (s, CH), (5.90, 5.92, 2 s, O-C$\underline{H_2}$-O), 6.07–8.20 [m, Ar (7H), CH = enolic], 9.29 (s, OH enolic), ^{13}C-NMR (100 MHz, $CDCl_3$) δ = 27.25–55.44 (10 aliphatic C), 101.25 (O-CH_2-O), 111.13–160.43 [6C = (Olefinic) + 10C Ar],197.84 (C=O), 198.55 (C=O). MS (EI) *m/z* (%): 470 (10) [M^+]; Anal. calcd. For: $C_{29}H_{30}N_2O_4$; (470.57); C, 74.02; H, 6.43; N, 5.95. Found: C, 73.98; H, 6.38; N, 5.90%.

10-(Benzo[d][1,3]dioxol-5-yl)-9-(4-chlorophenyl)-3,4,6,7-tetrahydro-3,3,6,6-tetramethylacridine-1,8(2H,5H,9H,10H)-dione (5e)

IR (KBr): 1630 (C=O), 1626 (C=O) cm^{-1}, ^1H-NMR (500 MHz, $CDCl_3$) δ ppm: 1.11–1.25 (s, $4CH_3$), 2.18, 2.22 (s, $2CH_2$), 2.38, 2.50 (s, $2CH_2$), 5.14 (s, CH), (5.85, 5.88, 2 s, O-C$\underline{H_2}$-O), 5.85–6.64 [m, Ar (3H)], 7.07–7.08 [d, J = 5 Hz, Ar (2H)], 7.46–7.47[d, J = 5 Hz, Ar(2H)], ^{13}C-NMR (100 MHz, $CDCl_3$) δ = 27.2–55.4 (11 aliphatic C), 101.25 (O-CH_2-O), 109.54–159.43 [4C = (Olefinic) + 12C Ar], 194.44 (C=O), 197.71 (C=O). MS (EI) *m/z* (%): 505 (20) [M^+ + 2]; 503 (23) [M^+]. Anal. calcd. For. $C_{30}H_{30}ClNO_4$; (503.93); C, 71.49; H, 5.99; N, 5.90; Found: C, 71.45; H, 5.96, N, 5.87.

3 | RESULTS AND DISCUSSION

3.1 | Characterization of synthesized nano zeolites

3.1.1 | XRD experimental data

Figure 1 illustrates the XRD patterns of synthesized zeolite 4A NPs that show several sharp peaks at 7.16, 10.27, 12.44, 16.05, 21.60, 24.50, 27.3. 30.00, and 34.30 (degree) which are assigned to their corresponding Miller indices (*hkl*) reflection planes of the cubic crystalline system previously indexed by Zamani et al.[42] and Hasegawa et al.[42,43]

Zeolite 4A shows the same previously assigned pattern, which indicates that its structure is well preserved even after pulsed laser ablation.

3.1.2 | Fourier transform-infrared spectra

Figure 2 shows the FT-IR-normalized absorption spectrum of zeolite 4A samples with the following features:

1. A sharp band at 455 cm^{-1}, which is assigned to internal vibrations of (Si–O) and (Al–O) bending.

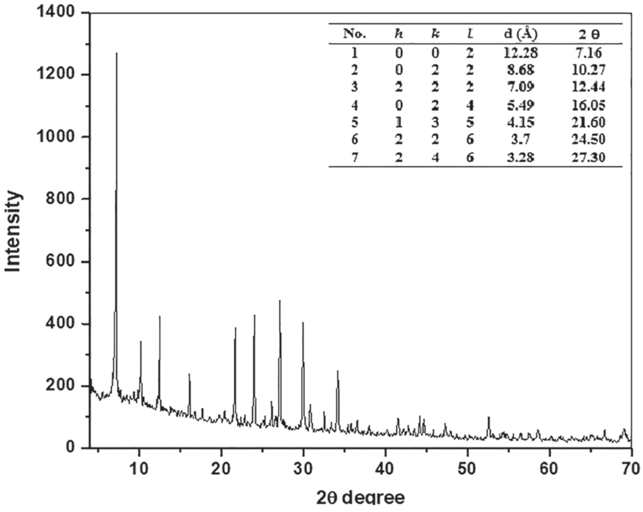

No.	*h*	*k*	*l*	d (Å)	2 θ
1	0	0	2	12.28	7.16
2	0	2	2	8.68	10.27
3	2	2	2	7.09	12.44
4	0	2	4	5.49	16.05
5	1	3	5	4.15	21.60
6	2	2	6	3.7	24.50
7	2	4	6	3.28	27.30

FIGURE 1 X-ray diffraction patterns of synthesized zeolite 4A nanoparticles

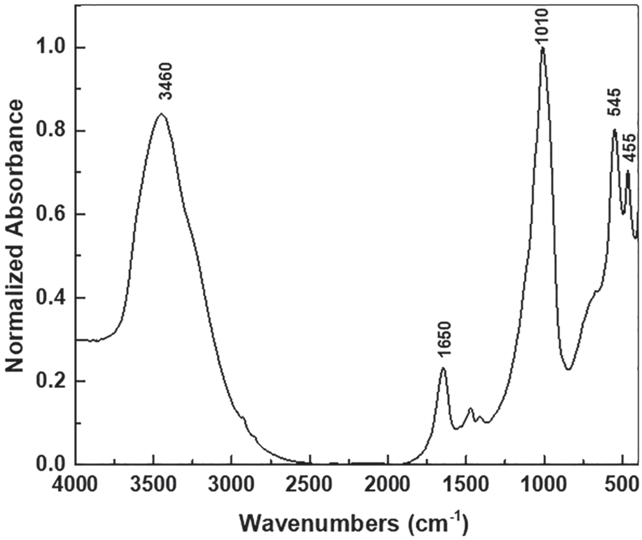

FIGURE 2 Fourier transform-infrared-normalized absorption spectrum of zeolite 4A

2. A sharp band at 554 cm^{-1}, which is assigned to the external vibration of double four rings.
3. A sharp intense band at 1010 cm^{-1}, which is attributed to asymmetric stretching vibrations of both silicon and aluminum atoms linked to the oxygen molecule.
4. A band centered at about 3460 cm^{-1}, along with that at 1665 cm^{-1}, both of which are related to OH groups.

3.1.3 | Scanning electron microscopy

Figure 3 shows the SEM micrograph of zeolite 4A samples after being treated with the laser beam. The figure reveals the presence of truncated-side cubic crystals with a size of about 25 nm, as calculated using the Debye–Scherrer equation and observed to be compatible with that observed on a transmission electron microscope.

Figure 4 shows the SEM mapping analysis of zeolite A4 samples studied. The obtained image reveals a homogenous distribution of all analyzed partner elements (Na, Mg, Al, Si, Ca, and O atoms) in their chemical structure (listed in Table 1 along with their atomic and weight percentages). Silica was the main

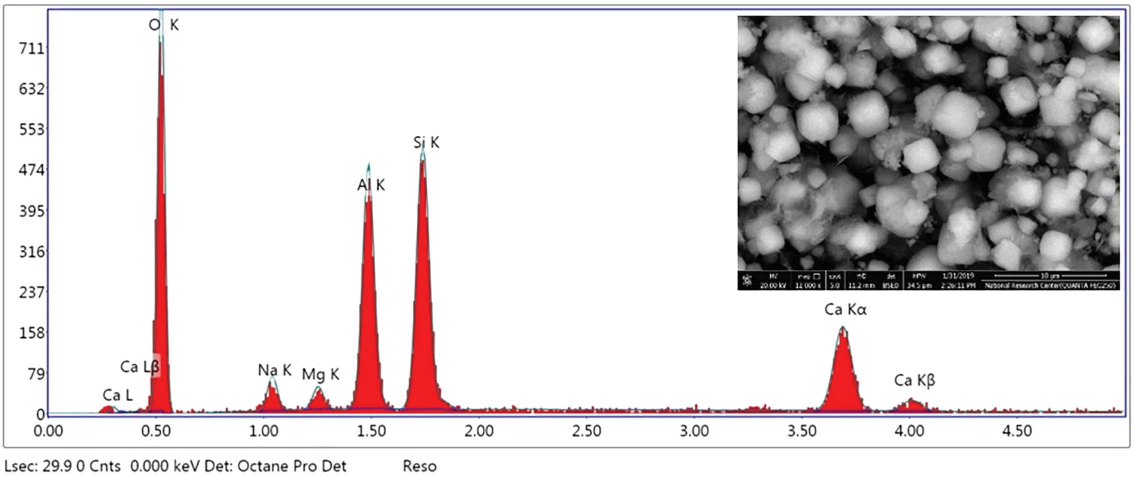

FIGURE 3 Scanning electron microscopy image (inset) with energy-dispersive X-ray analysis spectrum of zeolite 4A

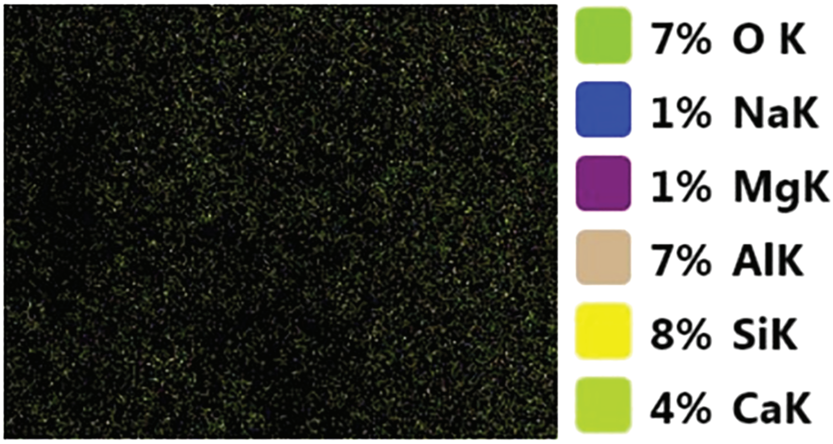

FIGURE 4 Scanning electron microscopy mapping of zeolite 4A

TABLE 1 Energy-dispersive X-ray analysis of studied sample

Element	Weight %	Atomic %
Na_2O	4.86	5.27
MgO	2.42	4.02
Al_2O_3	31.07	20.44
SiO_2	43.49	48.55
CaO	18.16	21.72

constituent, with lime and alumina comprising the major percentage, and soda and magnesium oxide constituting only a minor percentage.

3.1.4 | Transmission electron microscopy

Figure 5 shows TEM images with nearly homogenous spherical morphology. The average size of samples obtained from these observations ranges between 19 and 25 nm that matches well with that calculated from XRD experimental data. Furthermore, the selected area diffraction pattern of prepared nanocrystals shows a combined pattern of concentric rings and sharp bright spots over the rings, indicating a crystalline structure supporting XRD data.

3.2 | Organic synthesis

Multicomponent reactions are powerful strategies to synthesize important heterocyclic compounds with various important biological properties in an easy way using available materials.

The molecularly diverse structure of polynuclear and complex heterocyclic organic compounds makes them an important scaffold in many pharmaceutical applications. Xanthene derivatives, acridine derivatives, 1,4-dihydropyridine derivatives, and quinolone derivatives are good precursors in both organic synthesis and discovery of a new pharmaceutical substance.

Our group has developed many novel green methodologies for organic synthesis and transformations of compounds.[44–47] In continuation of our previous work, we report herein an efficient, facile, and powerful protocol for the one-pot synthesis of 1,8-dioxodecahydroxanthenes **(3a–3g)** and 1,8-dioxodecahydroacridines **(5a-5e)** using zeolite 4A NPs as a catalyst in aqueous reaction conditions. The synthesis involved the following steps:

1. A catalytic amount(10 mol%) of zeolite 4A NPs for an appropriateperiod(10–120 mins) prepared by treating, in deionized water, an aromatic aldehyde with 2 mol of dimedone in the presence of a

TABLE 2 Synthesis of 1,8-dioxo-octahydroxanthenes using various aldehydes

Entry	R_1	Product	Time (min)	Yield (%)
1	Phenyl	**3a**	20	80
2	4-Methoxyphenyl	**3b**	60	60
3	4-Chlorophenyl	**3c**	90	60
4	4-Fluorophenyl	**3d**	90	70
5	4-*N*,*N*-dimethylaminophenyl	**3e**	30	90
6	3-Pyridyl	**3f**	120	60
7	5-Nitro-2-furyl	**3g**	60	70

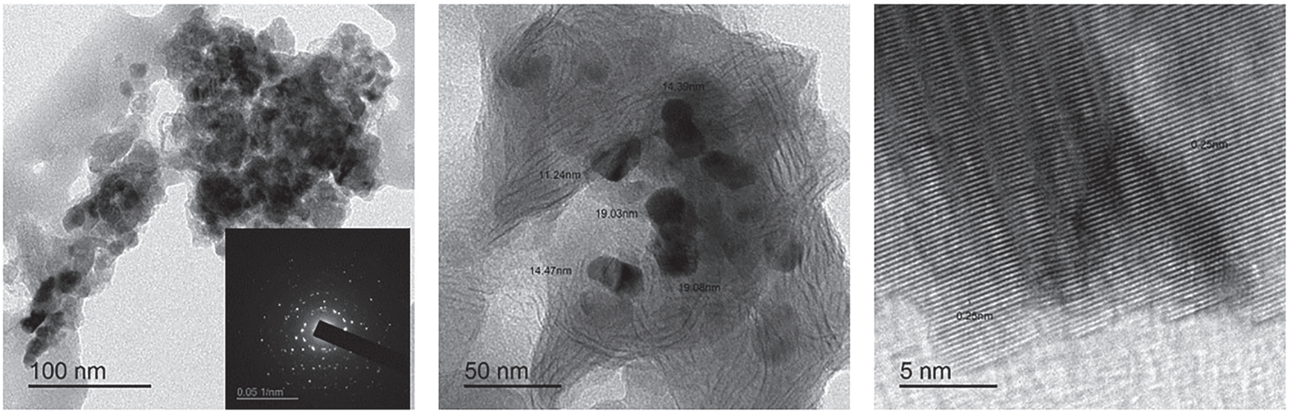

FIGURE 5 Transmission electron microscopy images, selected area diffraction pattern, and high-resolution image

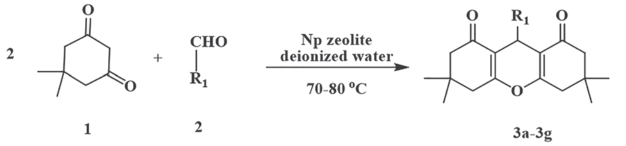

SCHEME 1 Synthesis of 1,8-dioxo-octahydroxanthenes. NP, nanoparticle

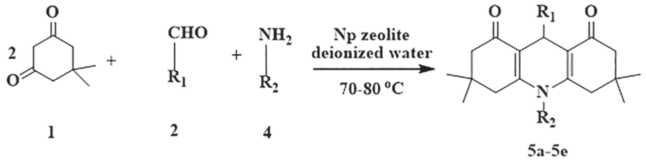

SCHEME 2 Four-component synthesis of *N*-aryl-1,8-dioxodecahydroacridines

catalytic amount of zeolite 4A NPs for an appropriate period. Upon formation of the final product, the reaction mixture was cooled down to room temperature and the catalyst filtered off using ethanol. The reaction was explored to understand the catalytic mechanism responsible for producing octahydroxanthenediones in high yield. Table 2 and Scheme 1 summarize the structures of the products, melting points, yield percentages, and reaction times for compounds **3a–3g.**

2. *N*-aryl-1,8-dioxodecahydroacridine derivatives were synthesized in a one-pot reaction using four components. The reaction was started by reacting 1 mol of aromatic amines and aromatic aldehydes and 2 mol of dimedone in the presence of a catalytic amount of zeolite NPs in deionized water at 70–80 °C. Within 10–30 min, *N*-aryl-1,8-dioxodecahydroacridines **(5a–5e)** are produced. The overall results are described in Table 3 and Scheme 2.

The proposed mechanism for the catalytic synthesis of octahydroxanthenediones is presented in Scheme 3. The aldehyde carbonyl group was polarized by the catalyst which facilitates the nucleophilic attack of C-2 of the enolized dimedone molecule, followed by that of another dimedone molecule to form intermediate I. This intermediate was then activated by the catalyst, which subsequently participates in another nucleophilic attack involving the lone pair of electrons of the OH group. Following the nucleophilic attack, dehydration occurred to produce the 1,8-dioxo-octahydroxanthene II.

3.3 | Molecular docking studies

In recent decades, molecular docking has become a progressively significant tool for drug discovery, as it can predict theoretically the interaction between a drug and a protein.[48–55] Such a method allows computational strategies to permeate all aspects of drug discovery, including virtual screening techniques, which are more direct and low in cost, compared with traditional experimental high-throughput screening.

Based on the standard docking protocol and using MOE 2015.10 software,[48] the docking between the synthesized 1,8-dioxo-octahydroxanthene (**3a–3g**) and *N*-aryl-1,8-dioxodecahydroacridine (**5a–5e**) compounds was validated using quinone reductase 2 (NQO2) as an inhibitor. For comparison, another reaction was performed using the same reactants, but with acridine orange as a ligand instead of NQO2. Historically, NQO2 was classified as a detoxification enzyme responsible for the reduction of potentially cytotoxic quinines.[49] In the presence of NQO2, the docking of the synthesized molecules occurred through the drug–ligand interaction on the “A” binding site in NQO2. The obtained results and the calculated binding energy score in kilocalories/mole (kcal/mol) are summarized in Figures 6–8. Data obtained show that the binding sites in the targeted enzyme (NQO2) are attractive for the synthesized molecules, compared with those in the common ligand (acridine orange).

TABLE 3 Reaction of various anilines, various aldehydes, and dimedone

Entry	R_1	R_2	Products	Time (min)	Yield (%)
1	3(MeO)Ph	Ph	**5a**	20	95
2	4(Cl)Ph	Ph	**5b**	20	90
3	4(F)Ph	Ph	**5c**	10	92
4	3-Pyridyl	3,4-Methylendioxyphenyl	**5d**	25	78
5	4(Cl)Ph	3,4-Methylendioxyphenyl	**5e**	30	75

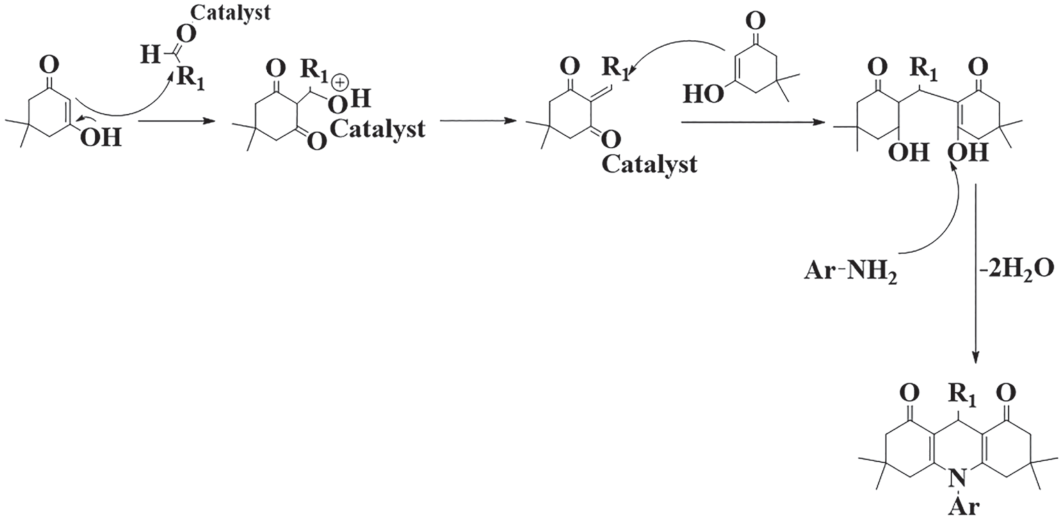

SCHEME 3 Proposed reaction mechanism

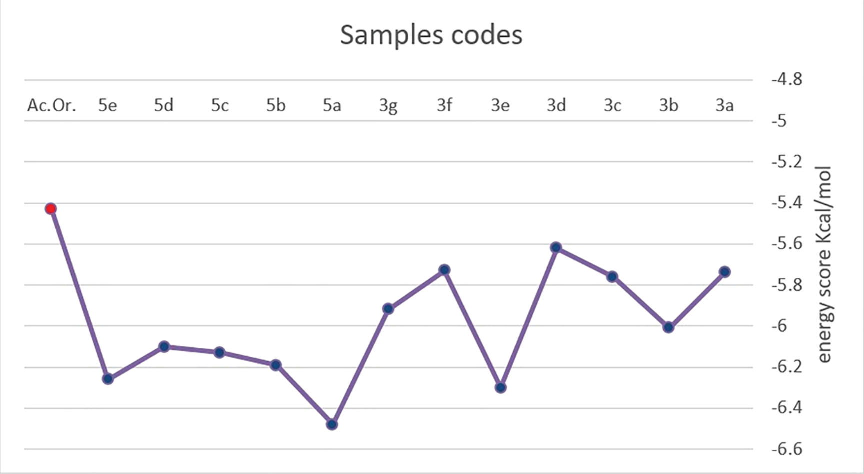

FIGURE 6 Calculated binding energy scores in kilocalories/mole (kcal/mol). The red point corresponds to acridine orange (reference sample) and black points to synthesized xanthenes and acridines

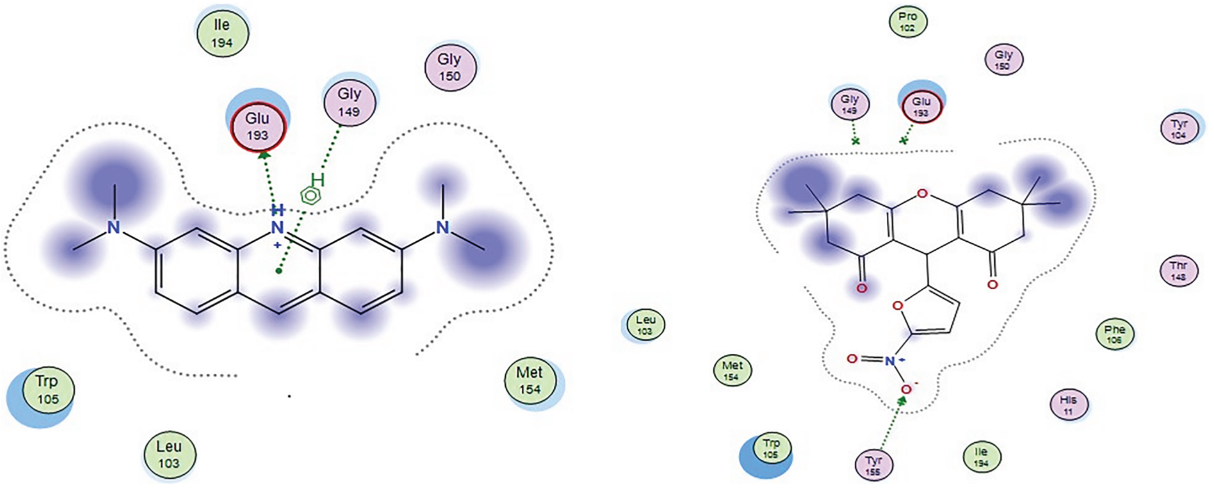

FIGURE 7 Two-dimensional interaction between pockets in quinone reductase 2 and **3g**, compared with that between **3g** and acridine orange

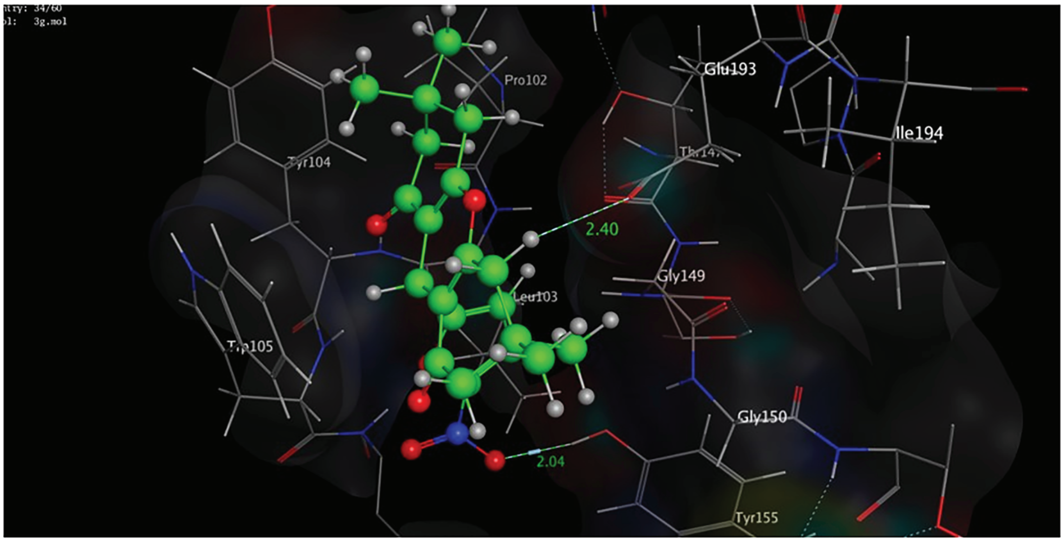

FIGURE 8 Three-dimensional interaction between pocket in quinone reductase 2 and compound **3g** with the hydrogen bond length indicated

4 | CONCLUSIONS

Zeolite NPs (molecular sieve 4A) were successfully produced by the PLAL technique. The potential of the heterogeneous catalyst (zeolite 4A NPs) was examined and characterized by FT-IR, XRD, FE-SEM, and HR-TEM. The catalyst zeolite 4A was then used for the synthesis of xanthene and acridine derivatives. The zeolite NPs proved to be an efficient, facile, and eco-friendly catalyst for the one-pot synthesis of 1,8-dioxo-octahydroxanthenes and 1,8-dioxo-octahydroacridines. Furthermore, results of molecular docking studies indicated that most synthesized molecules showed good drug–ligand interaction on the active site of NQO2, compared with that of acridine orange.

ORCID

A.M. Abdelghany https://orcid.org/0000-0001-8953-0056

REFERENCES

[1] A. Berghout, D. Tunega, A. Zaoui, *Clays Clay Miner.* **2010**, *58*(2), 174.

[2] A. Dutta, J. A. Schaidle, D. Humbird, F. G. Baddour, A. Sahir, *Top. Catal.* **2016**, *59*(1), 2.

[3] A. Julbe, M. Drobek, *Encyclopedia of Membranes*, Springer-Verlag Berlin Heidelberg, **2016** 2055.

[4] A. Garcia, C. M. Lopez, L. V. Garcia, J. Casanova, M. R. Goldwasser, *Ing. Invest.* **2016**, *36*(1), 62.

[5] N. Iwasaki, M. Kato, T. Ogawa, M. Hosoi, U.S. Patent Application no. 15/520, **2017**, 985.

[6] Q. Li, R. D. Partridge, U.S. Patent Application No. 14/966, **2016**, 407.

[7] M. A. Morsi, A. Rajeh, A. A. Menazea, *J. Mater. Sci. Mater. Electron.* **2019**, *30*(3), 2693.

[8] I. S. Elashmawi, A. A. Menazea, *J. Mater. Res. Technol.* **2019**, *2*(8), 1944.

[9] F. H. Abd El-kader, N. A. Hakeem, W. H. Osman, A. A. Menazea, A. M. Abdelghany, *Silicon* **2019**, *11*(1), 377.

[10] A. A. Menazea, A. M. Abdelghany, W. H. Osman, N. A. Hakeem, F. H. Abd El-Kader, *J. Non-Cryst. Solids* **2019**, *513*, 49.

[11] A. A. Menazea, A. M. Abdelghany, N. A. Hakeem, W. H. Osman, F. H. Abd El-kader, *Silicon* **2018**, 1. https://doi.org/10.1007/s12633-019-0094-3

[12] F. H. Abd El-kader, N. A. Hakeem, I. S. Elashmawi, A. A. Menazea, *Spectrochim. Acta A Mol. Biomol. Spectrosc.* **2015**, *138*, 331.

[13] A. A. Menazea, I. S. Elashmawi, F. H. Abd El-kader, N. A. Hakeem, *J. Inorg. Organomet. Polym. Mater.* **2018**, *28*, 2564.

[14] M. Dawy, H. M. Rifaat, A. A. Menazea, *Cur. Sci. I.* **2015**, *4*, 621.

[15] L. Ngadi, A. M. Galy, J. P. Galy, J. Barbe, A. Cremieux, J. Chevalier, D. Sharples, *Eur. J. Med. Chem.* **1990**, *25*(1), 67.

[16] S. Girault, P. Grellier, A. Berecibar, L. Maes, E. Mouray, P. Lemiere, M. A. Debreu, E. Davioud-Charvet, C. Sergheraet, *J. Med. Chem.* **2000**, *43*(14), 2646.

[17] Y. Mikata, M. Yokoyama, K. Mogami, M. Kato, I. Okura, M. Chikira, S. Yano, *Inorg. Chim. Acta* **1998**, *279*(1), 51.

[18] S. A. Gamega, J. A. Spicer, G. J. Atwell, G. J. Finlay, B. C. Baguley, W. A. Deny, *J. Med. Chem.* **1999**, *42*(13), 2383.

[19] M. Wainwright, *J. Antimicrob. Chemother.* **2001**, *47*(1), 1.

[20] P. Murugan, P. Shanmugasundaram, V. T. Ramakrishnan, B. Venkatachalapathy, N. Srividya, P. Ramamurthy, K. Gunasekaran, D. Velmurugan, *J. Chem. Soc., Perkin Trans.* **1998**, *2*, 999.

[21] A. Islam, P. Murugan, K. C. Hwang, C. H. Cheng, *Synth. Met.* **2003**, *139*(2), 347.

[22] F. Bossert, W. Vater, *Med. Res. Rev.* **1989**, *9*(3), 291.

[23] O. Berkan, B. Sarac, R. Simsek, S. Yildirim, Y. Sariogli, C. Safak, *Eur. J. Med. Chem.* **2002**, *37*(6), 519.

[24] S. Kantevari, R. Bantu, L. Nagarapu, *J. Mol. Catal. A: Chem.* **2007**, *269*(1–2), 53.

[25] Z. H. Zhang, Y. H. Liu, *Cat. Com.* **2008**, *9*(8), 1715.

[26] M. Seyyedhamzeh, P. Mirzaei, A. Bazgir, *Dyes Pigm.* **2008**, *76*(3), 836.

[27] B. Das, P. Thirupathi, K. R. Reddy, B. Ravikanth, L. Nagarapu, *Cat. Com.* **2007**, *8*(3), 535.

[28] H. Y. Lu, J. J. Li, Z. -H. Zhang, *Appl. Organomet. Chem.* **2009**, *23*(4), 165.

[29] A. A. Bakibaev, V. D. Fillimonov, E. S. Nevgodova, *Russ. J. Org. Chem.* **1991**, *27*, 1519.

[30] A. V. Chate, U. B. Rathod, J. S. Kshirsagar, P. A. Gaikwad, K. D. Mane, P. S. Mahajan, M. D. Nikam, C. H. Gill, *Chin. J. Catal.* **2016**, *37*(1), 146.

[31] N. Martin, M. Quinteiro, C. Seoane, J. L. Soto, A. Mora, M. Suarez, E. Ochoa, A. Morales, J. R. Del Bosque, *J. Heterocyclic Chem.* **1995**, *32*(1), 235.

[32] S. S. Tu, F. Fang, S. Zhu, T. Li, X. Zhang, Q. Zhuang, *J. Heterocyclic Chem.* **2004**, *41*(5), 767.

[33] S. J. Tu, Z. Lu, D. Shi, C. Yao, Y. Gao, C. Guo, *Synth. Commun.* **2002**, *32*(14), 2181.

[34] B. Das, P. Thirupathi, I. Mahender, V. S. Reddy, Y. K. Rao, *J. Mol. Catal. A: Chem.* **2006**, *247*(1–2), 233.

[35] B. Maleki, R. Tayebee, M. Kermanian, S. Sedigh-Ashrafi, *J. Mex. Chem. Soc.* **2013**, *57*(4), 290.

[36] S. Babadoust, *Int. J. Chem. Biomol. Sci.* **2014**, *6*, 72.

[37] S. Balalaie, F. Chadegani, F. Darviche, H. R. Bijanzadeh, *Chin. J. Chem.* **2009**, *27*(10), 1953.

[38] H. Naeimi, Z. S. Nazifi, *J. Nanopart. Res.* **2013**, *15*(11), 2026.

[39] S. S. Kahandal, A. S. Burange, S. R. Kale, P. Prinsen, R. Luque, R. V. Jayaram, *Cat. Com.* **2017**, *97*, 138.

[40] M. Dabiri, M. Baghbanzadeh, E. Arzroomchilar, *Cat. Com.* **2008**, *9*(5), 939.

[41] W. Shen, L. M. Wang, H. Tian, J. Tang, J. J. Yu, *J. Fluorine Chem.* **2009**, *130*(6), 522.

[42] F. Zamani, M. Rezapour, S. Kianpour, *Bull. Korean Chem. Soc.* **2013**, *34*(8), 2367.

[43] K. Hasegawa, E. Nishibori, M. Takata, M. Sakata, N. Togashi, J. Yu, O. Terasaki, *Jpn. J. Appl. Phys.* **1999**, *38*(S1), 65.

[44] T. K. Khatab, A. M. Abdelghany, H. A. Soliman, *Appl. Organomet. Chem.* **2019**, *33*, e4783.

[45] T. K. Khatab, A. M. Abdelghany, N. Shaker, Y. Osama, E. M. Kandil, *Silicon* **2018**, *10*(5), 2173.

[46] T. K. Tamer, A. El-Mekabaty, Z. M. Gamala, E. M. Kandil, *Egypt. J. Chem.* **2018**, *4*(61), 661.

[47] H. A. Soliman, T. K. Khatab, *Silicon* **2018**, *10*(2), 229.

[48] The Molecular Operating, E.; Chemical Computing Group I.; Montreal QC. In.**, 2016.**

[49] K. K. Leung, B. H. Shilton, *Biochemistry* **2015**, *54*(51), 7438.

[50] K. Kuca, K. Musilek, D. Jun, J. Zdarova-Karasova, E. Nepovimova, O. Soukup, M. Hrabinova, J. Mikler, T. C. Franca, E. F. F. Da Cunha, A. A. De Castro, M. Valis, T. C. Ramalho, *BMC Pharmacol. Toxicol.* **2018**, *19*, 8.

[51] W. E. A. de Lima, A. F. Pereira, A. A. de Castro, E. F. F. da Cunha, T. C. Ramalho, *Lett. Drug des. Discovery* **2016**, *13*(5), 360.

[52] A. da Silva Gonçalves, T. C. França, M. S. Caetano, T. C. Ramalho, *J. Biomol. Struct. Dyn.* **2014**, *32*(2), 301.

[53] W. E. Amaral de Lima, A. Francisco, E. F. F. da Cunha, Z. Radic, P. Taylor, T. C. C. França, T. C. Ramalho, *J. Biomol. Struct. Dyn.* **2017**, *35*(6), 1272.

[54] S. K. Jesudoss, J. J. Vijaya, K. Kaviyarasu, L. J. Kennedy, R. J. Ramalingam, H. A. Al-Lohedan, *RSC Adv.* **2018**, *8*(1), 481.

[55] S. K. Jesudoss, J. J. Vijaya, K. Kaviyarasu, P. I. Rajan, S. Narayanan, L. J. Kennedy, *J. Photochem. Photobiol. B Biol.* *186*(2018), 178.

How to cite this article: Abdelghany AM, Menazea AA, Abd-El-Maksoud MA, Khatab TK. Pulsed laser ablated zeolite nanoparticles: A novel nano-catalyst for the synthesis of 1,8-dioxo-octahydroxanthene and *N*-aryl-1,8-dioxodecahydroacridine with molecular docking validation. *Appl Organometal Chem*. 2019;e5250. https://doi.org/10.1002/aoc.5250